ACS central science

http://pubs.acs.org/journal/acscii

Research Article

Natural-Product-Directed Catalytic Stereoselective Synthesis of Functionalized Fused Borane Cluster–Oxazoles for the Discovery of Bactericidal Agents

Rajesh Varkhedkar,[‖] Fan Yang,[‖] Rakesh Dontha,[‖] Jianglin Zhang, Jiyong Liu, Bernhard Spingler, Stijn van der Veen,* and Simon Duttwyler*

Cite This: *ACS Cent. Sci.* 2022, 8, 322–331

Read Online

ACCESS | Metrics & More | Article Recommendations | Supporting Information

ABSTRACT: The identification of an alternative chemical space in order to address the global challenge posed by emerging antimicrobial resistance is very much needed for the discovery of novel antimicrobial lead compounds. Boron clusters are currently being explored in drug discovery due to their unique steric and electronic properties. However, the challenges associated with the synthesis and derivatization techniques of these compounds have limited their utility in the rapid construction of a library of molecules for screening against various biological targets as an alternative molecular platform. Herein, we report a transition-metal-catalyzed regioselective direct B–H alkylation–annulation of the *closo*-dodecaborate anion with natural products such as menthol and camphor as the directing groups. This method allowed the rapid construction of a library of 1,2,3-trisubstituted clusters, which were evaluated in terms of their antibacterial activity against WHO priority pathogens. Several of the synthesized dodecaborate derivatives displayed medium- to high-level bactericidal activity against Gram-positive and Gram-negative bacteria.

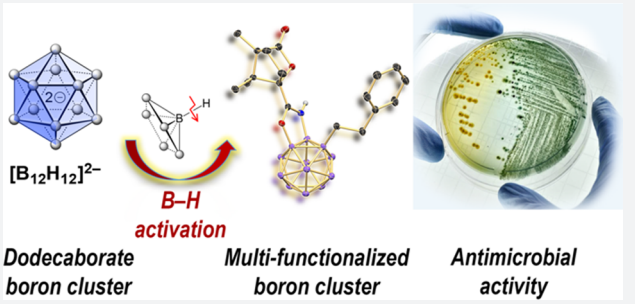

INTRODUCTION

The discovery of novel bioactive molecules is essential to overcome the impending challenges posed by emerging infectious diseases caused by multidrug-resistant pathogens worldwide.[1−4] The availability of antibiotics without prescription and their prophylactic use have spurred resistance, and bacteria of concern are, among others, *Staphylococcus aureus*, *Escherichia coli*, *Salmonella* spp. and *Neisseria gonorrhoeae*.[5] The Center of Disease Control antibiotic resistance threat report 2019 disclosed more than 2.8 million cases of antibiotic-resistant infections with more than 35000 fatalities in the US every year.[6] Research toward the discovery of antimicrobial agents is not attractive to pharmaceutical companies due to low profits and the limited lifespan associated with antibiotics, resulting in drying up of the corresponding pipeline and the risk of returning to the preantibiotic era.[7] In addition, studies of resistance mechanisms suggest high chances of mutations, leading to the ineffectiveness of well-established compounds.[8] Strategies to address this challenge involve the chemical modification of natural products as well as existing drugs.[9] Historically, screening of secondary metabolites obtained from microorganisms has been a primary source of bioactive molecules that prevent the growth of pathogens.[10] Studies on the biosynthesis of metabolites, probes of unexplored strains of microorganisms, and the availability of genome mining tools to activate silent gene clusters have yielded numerous antibacterial compounds.[11−13] Currently marketed drugs involve aminoglycosides, β-lactams, glycopeptides, polymyxins, and the corresponding semisynthetic derivatives.[14−16] Additionally, molecules bearing oxazolidinone, pyrimidine, quinolone, and sulfa functionalities have provided antibacterial candidates.[17,18]

The chemical space of natural products primarily comprises chiral compounds, whereas synthetic libraries often consist of flat aromatic molecules.[19] Icosahedral boron-rich clusters exhibit a spherelike distribution of electron density and can be compared to classical arenes.[20−27] Combining natural products with boron clusters can therefore enable access to a unique chemical space for the discovery of novel bioactive molecules. The *closo*-dodecaborate dianion $[B_{12}H_{12}]^{2-}$ is a highly symmetrical molecule, and the installation of three different substituents leads to R_{cage}-**1** and S_{cage}-**1** stereoisomers (Figure 1a). The chirality due to such cage substitution has the potential for applications in designing molecules for medicinal

Received: September 22, 2021
Published: February 11, 2022

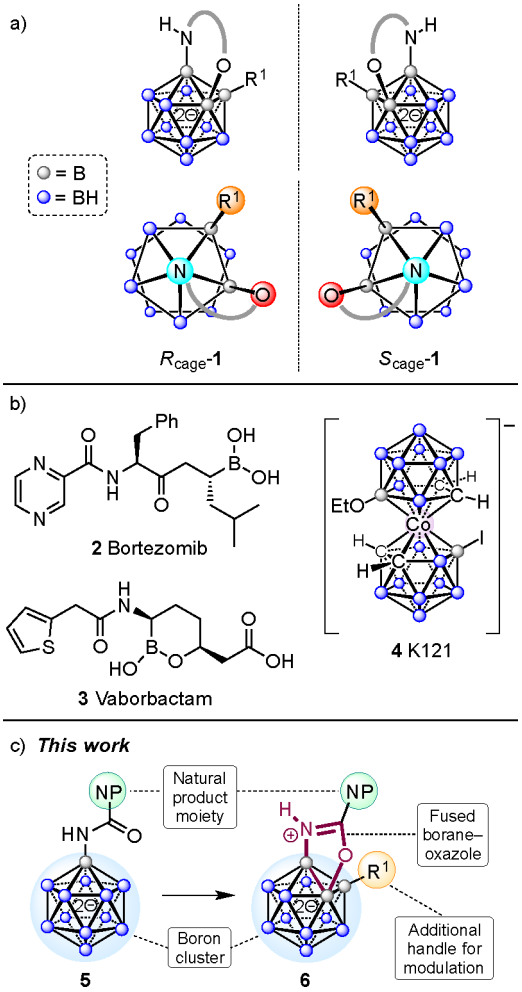

Figure 1. (a) Cage chirality of 1,2,3-trisubstituted *closo*-dodecaborates. (b) Boron-containing bioactive compounds. (c) Design of functionalized dodecaborates in this study. Color code: gray spheres, B; blue spheres, B–H.

chemistry, asymmetric synthesis, and materials science. However, there are limited reports on the enantioselective synthesis of such chiral compounds, and their utility has not been explored.[28−31]

The incorporation of boron as a part of bioactive compounds has recently gained much interest.[32−35] Several boron-containing compounds are in clinical use, such as bortezomib (**2**), a proteasome inhibitor, and vaborbactam (**3**), an antibiotic (Figure 1b).[36−38] Boron clusters are relatively nontoxic pharmacophores with steric and electronic properties that set them apart from organic building blocks.[39−43] Studies on their medicinal applications have focused on boron neutron capture therapy (BNCT) and on the inhibition of enzymes. On the other hand, their antimicrobial properties have been investigated only to a limited degree.[44] In an early review article on the potential applications of boron clusters, Plešek postulated that derivatives resembling known antibiotics may be promising drug analogues that cannot easily be degraded by pathogens.[45] Examples where polyhedral boron moieties seem to play a crucial role in antibacterial activity are the metallacarboranes: e.g., the bis(dicarbollide) K121 (**4**; Figure 1b).[46] Recently, the groups of Šicha and Viñas have probed related compounds to that end.[47−50] In 2020, Spokoyny reported on the synthesis and properties of the borane–saccharide hybrid $[B_{12}(OCH_2C_6H_4\text{-}1\text{-thio-D-galactose})_{12}]^{2-}$, which exhibits strong binding affinity to the B subunit of Shiga toxin 1.[51] Our own group has found that fused 2D/3D heterocycles based on the $[B_{12}H_{12}]^{2-}$ framework possess antimicrobial properties.[52] We therefore wondered whether *closo*-dodecaborates comprising a fused N,O-heterocycle and an additional group at a boron vertex would show similar effects. Amides **5** were anticipated to serve as starting materials for the target compounds **6**, which can be viewed as 3D analogues of benzoxazoles with an organic handle R^1 (Figure 1c). This strategy requires double B–H activation, including B–C bond formation and B–O annulation. The synthesis of functionalized polyhedral boranes and carboranes by B–H activation has emerged as a powerful tool,[53−58] but derivatization of anionic $\{CB_{11}\}$ and $\{B_{12}\}$ clusters has only been accomplished in recent years.[59−64] For dodecaborates, ureido and amide functionalities can serve as directing groups to achieve B–C and concomitant B–O bond formation.[61,64]

A major challenge for the transformation **5** → **6** was the choice of a suitable directing group. Our aim was to use a motif that provides the possibility to explore cage chirality as well as antimicrobial properties. S_{cage}/R_{cage} stereoinduction required a substituent with saturated stereogenic centers close to the transition metal and boron vertices in the relevant transition state(s). However, aliphatic amides have not been explored in dodecaborate B–H activation. We decided to focus on directing groups involving (−)-menthol and (−)-camphanic acid on the basis of their rigid alicyclic structure, commercial availability, and reported bioactivities.[65,66] We herein present a transition-metal-catalyzed, fully regioselective alkylation–annulation reaction for the construction of fused diboraoxazoles of the *closo*-dodecaborate cluster by using the aforementioned directing groups and alkene coupling partners. The method enabled the synthesis of a library of diversity-oriented boron clusters **13** and **14** under mild conditions in good yields and moderate to high stereoselectivity. Antibacterial properties were observed for several molecules of the series **13** and **14**, thus suggesting that multiply functionalized fused *closo*-dodecaborates represent a feasible alternative chemical space to traditional frameworks of organic antibiotics. Notably, one of the compounds, **14k**, was found to be active with a minimum inhibitory concentration (MIC) of up to 4 μM against Gram-positive *S. aureus* and *Enterococcus faecalis* and an MIC of up to 2 μM against Gram-negative *N. gonorrhoeae*.

RESULTS AND DISCUSSION

The design of target compounds **6** required directing groups that allow for stereoselective B–H activation of the dodecaborate cage and also possess bioactivity on their own. We selected amides of (−)-camphanic acid and (−)-menthyl carbonate as directing groups, which fulfill the following desirable criteria: (1) they possess a rigid structure with nonracemizing stereogenic centers, (2) they contain a functional group with the ability to coordinate to a transition metal to initiate B–H activation, (3) they can be easily installed on the boron cluster, and (4) they do not undergo side reactions. We anticipated $[B_{12}H_{12}(NH_3)]^-$ to serve as a convenient cluster starting material enabling facile amide bond formation.[52] Thus, $[B_{12}H_{12}(NH_3)]^-$ was treated with 3 equiv of NaH in THF for complete deprotonation of the NH_3 moiety, followed by combination with 1.1 equiv of (−)-camphanic acid chloride (**8**) or (−)-menthyl chlorocarbonate (**9**) (Scheme 1). The reactions were carried out at 25

https://doi.org/10.1021/acscentsci.1c01132
ACS Cent. Sci. 2022, 8, 322−331

Scheme 1. Acylation of $[B_{12}H_{11}NH_3]^-$ Providing Camphanyl Amide 10 and Menthyl Amide 11

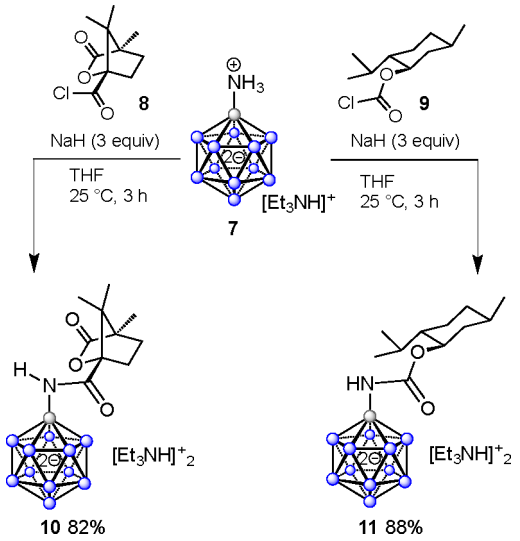

°C for 2 h under anhydrous conditions and subsequently quenched with a saturated aqueous solution of $[Et_3NH]Cl$. The amidations provided products **10** and **11** in 82% and 88% yields, respectively, after purification by column chromatography. Compounds **10** and **11** were fully characterized by multinuclear NMR spectroscopy and mass spectrometry.

Single crystals of the composition $[\mathbf{10}]_2[Et_3NH]_4\cdot$(acetone) suitable for X-ray diffraction were obtained from acetone–hexane at room temperature. The solid-state structure revealed the distances (Å) B1–N1 1.525(4), N1–C1 1.316(4), C1–O1 1.239(3), and C1–C2 1.516(3) (Figure 2). The structural

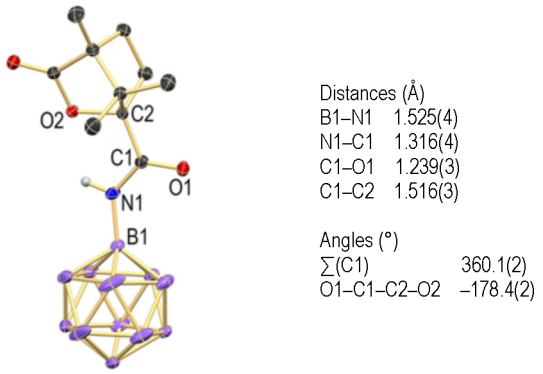

Figure 2. X-ray crystal structure of $[\mathbf{10}]_2[Et_3NH]_4\cdot$(acetone) (only one of the two anions in the asymmetric unit is shown; 25% displacement ellipsoids; cations, acetone solvent molecule, and hydrogen atoms except for N–H are omitted for clarity).

features are similar to those of typical organic amides; in particular, the coordination geometry around C1 is trigonal planar with a sum of angles of 360.1(2)° around this atom. The oxygen atoms O1 and O2 adopt a transoid geometry with respect to the C1–C2 axis, as indicated by the torsion angle of −178.4(2)° for O1–C1–C2–O2. Overall, the structure is similar to that of the closely related dodecaborate amide $[B_{12}H_{11}(NH)(CO)(\text{thiophen-2-yl})]^-$.[52]

Upon attaching the desired directing groups to the *closo*-dodecaborate cage, we evaluated transition-metal-catalyzed coupling to explore the feasibility of formation of compounds **6**. Initially, we investigated the B–H activation of **10** with styrene (**12a**) in the presence of Rh or Ir catalysts. A reaction with $[Cp^*RhCl_2]_2$ or $[Cp^*IrCl_2]_2$ (10 mol %) at 25 or 60 °C for 24 h indicated only a trace of the desired product by ESI-MS and mostly unchanged starting material (Table 1).

Table 1. Optimization of the Alkylation–Annulation Reaction[a]

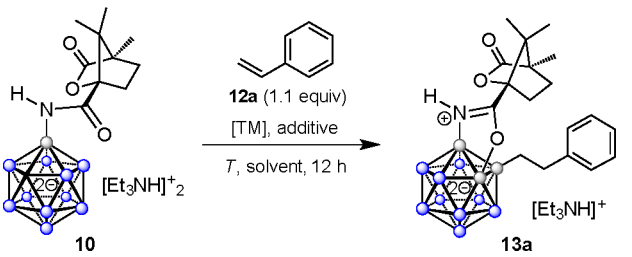

no.	[TM][b] (amt, mol %)	additive (amt, equiv)[c]	T (°C)	solvent	yield (%)
1	[Rh] (10)		60	MeCN	
2	[Ir] (10)		60	MeCN	
3	[Rh] (10)	[Cu] (2)	60	MeCN	50
4	[Rh] (10)	[Ag] (1)	60	MeCN	
5	[Ir] (10)	[Cu] (2)	60	MeCN	50
6	[Ir] (10)	[Ag] (1)	60	MeCN	
7	[Ir] (10)	[Cu] (2)	40	MeCN	65
8	[Rh] (10)	[Cu] (2)	40	MeCN	75
9	[Rh] (5)	[Cu] (2)	25	MeCN	82
10	[Ir] (5)	[Cu] (2)	25	MeCN	72
11	**[Rh] (2.5)**	**[Cu] (2)**	**25**	**MeCN**	**85**
12	[Rh] (2.5)	[Cu] (2)	25	EtOH	
13	[Rh] (2.5)	[Cu] (2)	25	Acetone	52
14	[Rh] (2.5)	[Cu] (2)	25	MeOH	
15	[Rh] (2.5)	[Cu] (2)	25	THF	56
16	[Rh] (2.5)	[Cu] (2)	25	DCE	48

[a]Reactions were conducted on a 20 mg scale in 1 mL of the solvent in a glass vial sealed with a screw cap. [b]Definitions: [Rh], $[RhCp^*Cl_2]_2$; [Ir] = $[IrCp^*Cl_2]_2$. [c]Definitions: [Cu], $Cu(OAc)_2\cdot H_2O$; [Ag] = AgOAc.

Therefore, we tried addition of $Cu(OAc)_2$ and AgOAc. The reaction of **10** in the presence of $[Cp^*RhCl_2]_2$ or $[Cp^*IrCl_2]_2$ and $Cu(OAc)_2\cdot H_2O$ (2 equiv) at 60 °C suggested more than 50% conversion along with a mixture of other compounds by MS, whereas using AgOAc as an additive was not found to be helpful. Thus, we lowered the temperature as well as catalyst loading. The reaction of **10** in the presence of $[Cp^*RhCl_2]_2$ or $[Cp^*IrCl_2]_2$ and $Cu(OAc)_2\cdot H_2O$ (2 equiv) at 40 °C significantly improved the yield of the desired product to up to 65–75%. Further lowering of the catalyst loading and temperature to 2.5 mol % at 25 °C furnished the desired product in 85% yield upon isolation by column chromatography. The reaction in other solvents such as acetone, THF, and DCE gave yields of 56% or less. EtOH or MeOH afforded primarily unchanged starting materials.

From these screening experiments, entry 11 of Table 1 was used as the basis for transformations on a larger scale and an exploration of the substrate scope. Under these conditions, we performed the reaction of **10** with **12a** on a 200 mg scale to give the corresponding product **13a** in 85% yield after purification by column chromatography. ^1H NMR spectroscopy and mass spectrometry suggested reductive coupling of **10** with **12a**, leading to a B–$(CH_2)_2$–Ph moiety. ^{11}B and $^{11}B\{^1H\}$

https://doi.org/10.1021/acscentsci.1c01132
ACS Cent. Sci. 2022, 8, 322–331

NMR spectra showed desymmetrization of the cage as well as characteristic, distinct resonances at 6.6, −4.5, and −10.2 ppm corresponding to B−O, B−N, and B−C vertices, respectively (Figure 3). This peak pattern was in full agreement with that observed for related dodecaborates in earlier studies.[61,64]

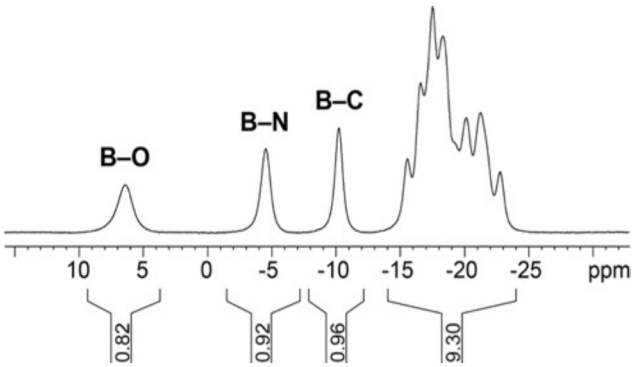

Figure 3. ^{11}B NMR spectrum of [Et_3NH][**13a**] (128 MHz, acetone-d_6, 23 °C).

Single crystals of **13a** were obtained from a H_2O/EtOH solution by slow evaporation of most of the EtOH over 21 days at room temperature. An X-ray diffraction analysis revealed the composition [**13a**]$_4$[Et_3NH]$_4$·5H_2O with four anions in the asymmetric unit (Figure 4). The cage showed the anticipated

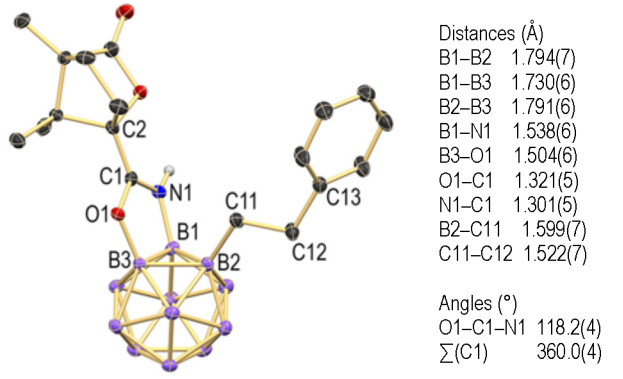

Figure 4. X-ray crystal structure of [**13a**]$_4$[Et_3NH]$_4$·5H_2O (only one of the four anions in the asymmetric unit is shown; 25% displacement ellipsoids; cations, H_2O solvent molecules, and hydrogen atoms except for N−H are omitted for clarity).

1,2,3-trisubstitution caused by B−C coupling and heterocycle generation upon B−O bond formation. All of the anions exhibited an R_{cage} configuration and similar structural features. Therefore, only one of them is described in detail in the following. The B1−B3 distance is 1.730(6) Å, slightly contracted in comparison to other B−B distances, indicative of electron delocalization within the diboraoxazole ring. Although this effect is not very strong, it is consistent with reports on similar compounds and all other distances within the ring.[52,61,64] The coordination around C1 is trigonal planar with an internal angle of O1−C1−N1 of 118.2(4)° and a sum of angles of 360.0(4)°. The C11−C12 distance of 1.522(7) Å confirmed reductive coupling with **12a**, resulting in a CH_2−CH_2 single bond.

Using the established protocol, we evaluated the generality of the reaction of **10** and **11** with various substituted styrenes as well as other olefins to generate a library of compounds. In general, the coupling−cyclization consistently provided access to products **13** and **14** in moderate to high yields under ambient conditions (Table 2). For all of the compounds, two sets of signals were observed in the ^{1}H and ^{13}C{^{1}H} NMR spectra (but not in the ^{11}B NMR spectra due to the naturally broadened signals), consistent with the formation of diastereomers featuring an unchanged absolute configuration of the directing group and R_{cage}/S_{cage} configuration at the cage. For **13a** and **14a**, 1D and 2D NMR experiments were performed to assign all ^{1}H and ^{13}C resonances. On the basis of this analysis, diagnostic signals were used to determine the diastereomeric ratios dr (see the Supporting Information for details). Although in each of the series **13** and **14** one diastereoisomer consistently dominated, at present we are unable to state whether this corresponds to the R_{cage} or the S_{cage} configuration.[67]

Substituted styrenes with electron-withdrawing and electron-donating functionalities furnished products **13a−k** and **14a−n** with very high regioselectivity and control over the degree of substitution as well as moderate to good diastereoselectivity. Minor undesired compounds were dialkylated species and trace amounts of unchanged starting material. Purification by chromatography afforded isolated yields of 63−92%. Typically, diastereomeric ratios were in the range of 60:40 to 80:20. Notably, higher values of up to 91:9 were observed for styrenes with 4-^{t}Bu and 4-OC(O)Me substitution (**13f,g** and **14f,g**). Coupling of **11** with the nonaromatic alkenes CH_2−CH−R (R = CO_2Me, $CO_2{}^t$Bu, $(CH_2)_9CH_3$) proceeded in high yields of 85−92% (**14l−n**). However, in these cases the dr was 1:1, suggesting that the nature of the alkene coupling partner plays a decisive role in the diastereodiscriminating step.

Our previous studies suggested that the alkylation−annulation cascade occurs via B−C coupling followed by B−O bond formation as the essential steps.[61,63] Both of these events require B−H activation, and several intermediates with B−H−Rh agostic-like and B−Rh direct interactions are likely to be involved. A proposed mechanism is displayed and discussed in pages S9 and S10 in the Supporting Information. Stereoinduction occurs in the second B−H activation step (affording the intermediates R_{cage}-**V** and S_{cage}-**V** in Scheme S2) and is governed by the absolute stereochemistry of the natural product moiety. Subsequently, B−O bond formation−cyclization generates R_{cage}-**13**/R_{cage}-**14** and S_{cage}-**13**/S_{cage}-**14** diastereomers. We intend to investigate the mechanistic manifold and the question as to which stereochemical outcome is preferred by the chiral directing groups with the assistance of calculations in a separate study.

To probe and compare the bioactivity of the trisubstituted boron clusters with that of disubstituted boron clusters, we carried out further transformations of **10** and **11**. Treatment with 1.1 equiv of the iodine(III) reagent (diacetoxyiodo)-benzene in MeOH gave the cyclized products **15** and **16** cleanly in 90% yield after silica gel chromatography (Scheme 2). The reaction proceeded under mild conditions in MeOH in air within 10 min, and no side reactions such as cage overoxidation and formation of B_{cage}−iodonium species were observed.

Antibacterial Activity. The antimicrobial activity of all synthesized compounds was evaluated against commonly encountered "problem germs", Gram-positive and Gram-negative antimicrobial-resistant bacteria that are defined in the WHO priority list (for the complete table of all tested

https://doi.org/10.1021/acscentsci.1c01132
ACS Cent. Sci. 2022, 8, 322−331

Table 2. Synthesis of Fused *closo*-Dodecaborate−Oxazoles[a]

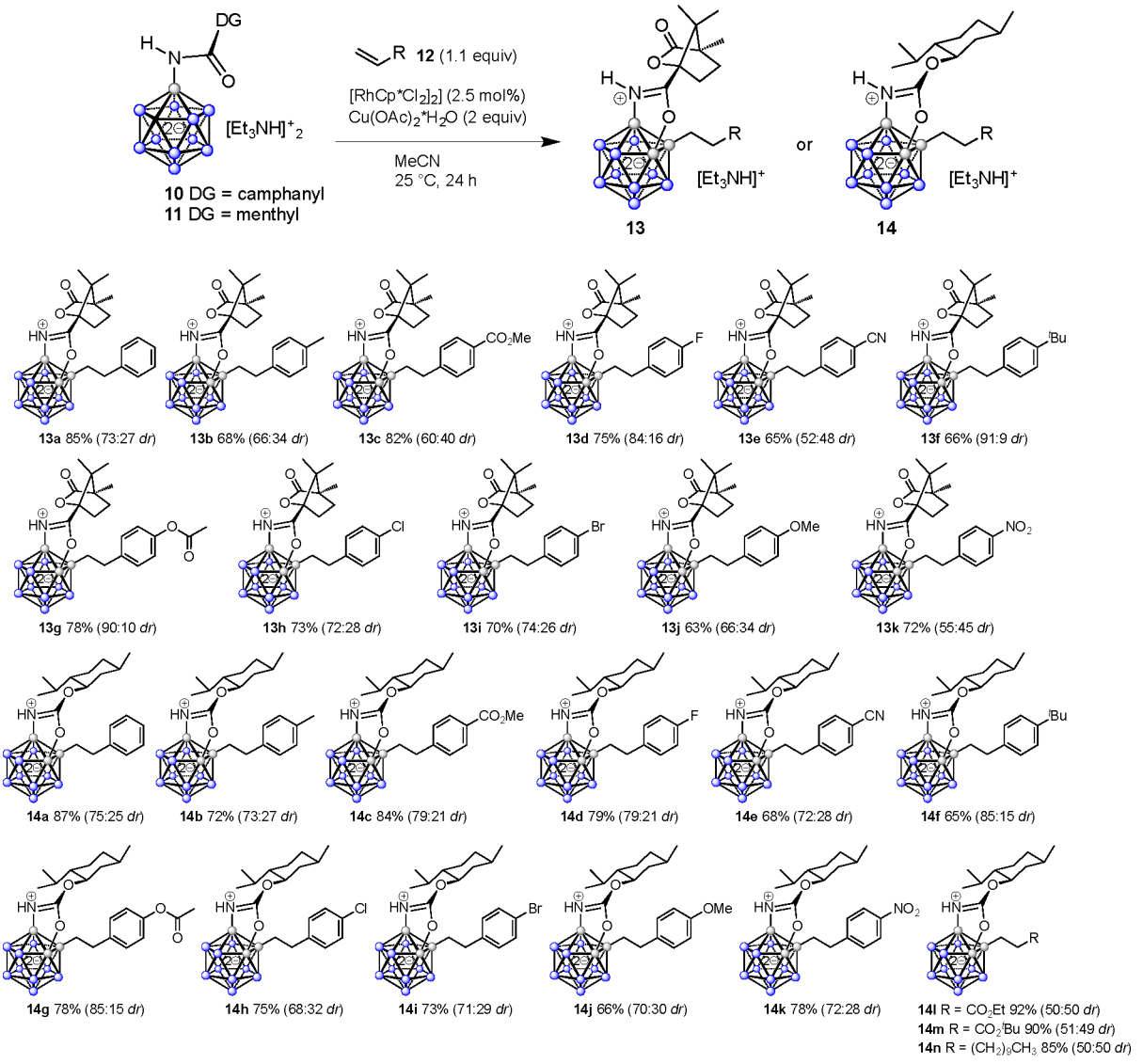

[a]Reactions were performed on a 100 mg scale in MeCN (5 mL) in a 20 mL glass vial with a screw cap. The yields noted are isolated yields after purification by chromatography. dr values were determined by NMR. See the Supporting Information for details.

Scheme 2. Synthesis of Cyclized Compounds 15 and 16

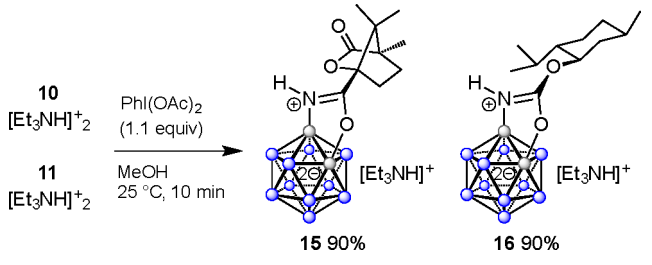

strains, see the Supporting Information).[68] The minimum inhibitory concentrations (MICs) of our compounds and the antibiotics ceftriaxone, azithromycin, and ciprofloxacin were determined against international reference strains *N. gonorrhoeae* ATCC 49226, *S. aureus* ATCC 25923, *E. faecalis* ATCC 29212, *Acinetobacter baumannii* ATCC 19606, *Klebsiella pneumonia* ATCC 700603, *Pseudomonas aeruginosa* ATCC 27853, *E. coli* ATCC 25922, *Enterobacter cloacae* ATCC 700323, *Stenotrophomonas maltophilia* ATCC 17666, *Listeria monocytogenes* EGDe, and *Shigella sonnei* SD10053 using the agar dilution method (see Table S1 in the Supporting Information). All compounds of the series **13** showed strong antimicrobial activity against the Gram-negative species *N. gonorrhoeae*, with compounds **13h,I** displaying the best activity at an MIC of 4 μM (Table 3). Most of the series **13** compounds furthermore displayed activity against the Gram-positive species *S. aureus* and *E. faecalis*, with the best activities being observed for compounds **13f,h,I**, which displayed MICs of 8−16 μM against *S. aureus* and 16−32 μM against *E. faecalis*. None of the series **13** compounds displayed activity against any of the other tested bacterial species (see Table S1 in the Supporting Information). Similarly, all of the series **14** compounds showed strong activity against *N. gonorrhoeae*, with the best activity being observed for compound **14k** at an MIC of 2 μM (Table 3). Most of the series **14** compounds also displayed strong activity against *S. aureus*, *E. faecalis*, and *L. monocytogenes*, with the most consistent activity against all

https://doi.org/10.1021/acscentsci.1c01132
ACS Cent. Sci. 2022, 8, 322−331

Table 3. MIC Data (μM) for Our Compounds against Selected Gram-Positive and Gram-Negative Bacteria

	Gram negative		Gram positive		
compound	*Neisseria gonorrhoeae* ATCC 49226	*Stenotrophomonas maltophilia* ATCC 17666	*Staphylococcus aureus* ATCC 25923	*Enterococcus faecalis* ATCC 29212	*Listeria monocytogenes* EGDe
10	>256	>256	>256	>256	>256
13a	16	>256	128	128	>256
13b	16	>256	32	64	>256
13c	16	>256	64	>256	>256
13d	8	>256	64	>256	>256
13e	16	>256	64	64	>256
13f	8	>256	8	16	>256
13g	64	>256	256	256	>256
13h	4	>256	16	32	>256
13i	4	256	16	16	>256
13j	32	>256	64	64	>256
13k	8	>256	64	64	>256
15	>256	>256	>256	>256	>256
11	128	>256	>256	>256	>256
14a	4	64	4	4	8
14b	8	64	8	8	16
14c	16	256	8	16	16
14d	8	32	4	8	8
14e	4	128	4	8	16
14f	8	256	16	16	16
14g	4	>256	4	32	32
14h	4	16	4	4	8
14i	4	32	4	4	4
14j	4	64	4	8	8
14k	2	>256	4	4	32
14l	4	128	8	16	>256
14m	4	128	8	8	>256
14n	16	>256	>256	64	>256
16	16	>256	64	128	>256
(−)-menthol	>256	>256	>256	>256	>256
(−)-camphanic acid	>256	>256	>256	>256	>256
$[Et_3NH][B_{12}H_{11}\text{-}NH_3]$	>256	>256	>256	>256	>256

Table 4. MIC Data (μM) for Selected Compounds and Marketed Antibiotics against Multidrug-Resistant Clinical Isolates of *Neisseria gonorrhoeae*

	compound																			
	13d	**13f**	**13h**	**13i**	**13k**	**14a**	**14b**	**14d**	**14e**	**14f**	**14g**	**14h**	**14i**	**14j**	**14k**	**14l**	**14m**	ceftriaxone	azithromycin	ciprofloxacin
N. gonorrhoeae ATCC 49226	8	8	4	4	8	4	8	8	4	8	4	4	4	4	**2**	4	4	0.008	0.016	0.03
N. gonorrhoeae ZJXSH 89	8	8	4	4	8	4	8	8	4	16	4	4	4	4	**2**	4	4	0.016	2048	48
N. gonorrhoeae ZJXSH 86	8	8	4	4	8	4	8	8	4	8	4	4	4	4	**2**	4	4	0.008	0.016	48

three species being observed for compound **14i** at an MIC of 4 μM. Antimicrobial activity was also observed against the Gram-negative species *S. maltophilia*, although to a lesser degree, with compound **14h** being most active with an MIC of 16 μM. No activity for the series **14** compounds was observed against the other tested bacterial species (see Table S1 in the Supporting Information). As a general trend, compounds containing the $-^t$Bu group, halides, or polar functionalities such as −OMe and $-NO_2$ within the aryl moiety feature higher effectivity. Importantly, the antimicrobial activity of the series **13** compounds was dependent on the additional arylethyl group of these trisubstituted compounds, since the disubstituted control compound **15** did not display any antimicrobial activity. In contrast, for the series **14** compounds the additional arylethyl group did not appear to be essential for activity against *N. gonorrhoeae*, *S. aureus*, and *E. faecalis*, albeit the activity of the disubstituted control compound **16** was lower than that observed for the trisubstituted compounds that contained the additional handle. Therefore, it appears that addition of the menthyl moiety, but not the camphanic acid moiety, was beneficial for antimicrobial activity, which might explain the overall better activity observed for the series **14** compounds. In the case of noncyclized amides **10** and **11**, no significant activity was detected. Similarly, the MIC values of the building blocks $[B_{12}H_{11}\text{-}NH_3]^-$, (−)-menthol, and (−)-camphanic acid were all >256 μM. This comparison

https://doi.org/10.1021/acscentsci.1c01132
ACS Cent. Sci. 2022, 8, 322−331

highlights the effect of the combination of the cluster−oxazole fusion with the additional B−C derivatization of the adjacent boron vertex position.

Compounds of series **13** and series **14** both showed particularly strong activity against the *N. gonorrhoeae* reference strain. *N. gonorrhoeae* has developed resistance against all of the previously and currently used antimicrobials, and due to the continued emergence of multidrug-resistant strains, infections with *N. gonorrhoeae* have become increasingly difficult or even impossible to treat successfully.[69,70] Resistance against the previously recommended antimicrobials ciprofloxacin and azithromycin is widespread, and susceptibility to the currently last available first-line therapy ceftriaxone is rapidly waning.[71−75] Therefore, it is of utmost importance to develop novel antimicrobials for this multidrug-resistant bacterial pathogen. Importantly, compounds of the series **13** and **14** also showed strong activity against two recent multidrug-resistant clinical isolates, with the susceptibility being almost identical with the susceptibility displayed by the reference strain (Table 4), indicating that the molecular target of these compounds is distinct from that of previously or currently used antimicrobials.

Generally, the activity of antimicrobials can be divided into bacteriostatic compounds, which inhibit growth but do not kill, and bactericidal compounds that are able to directly kill the bacteria. This distinction is clinically relevant, since bacteriostatic compounds are dependent on an active host immune response to clear the infection, which might be problematic in immunocompromised individuals or not rapid enough for infections of the central nervous system or the heart.[76,77] Therefore, we selected compound **14k**, which features a phenyl-nitro moiety that showed the lowest MIC values, and tested its mode of activity against *N. gonorrhoeae* and *S. aureus* in time-kill analyses. As controls, we included the currently recommended first-line bactericidal antibiotics ceftriaxone[69,70] and vancomycin[78] for comparison. Compound **14k** displayed rapid bactericidal activity against both *N. gonorrhoeae* and *S. aureus* (Figure 5). Exposure of *N. gonorrhoeae* to compound **14k** at 4 × MIC resulted in >100000-fold reduction in CFU counts within the first hour, whereas ceftriaxone required 8 h to achieve similar inactivation. Of note, the MIC of ceftriaxone against *N. gonorrhoeae* is 250-fold lower in comparison with compound **14k**, while the time-kill analyses were performed on the basis of relative × MIC values. In the case of *S. aureus*, exposure to compound **14k** at 4 × MIC caused a >100000-fold inactivation within the first 2 h, whereas vancomycin could not effectively achieve inactivation, even after 8 h of exposure. The time-kill assays, corroborated by the results of bacterial live/dead staining (Figure 5e), thus accentuate the strong potential of **14k** as a lead for novel antimicrobial compounds to treat bacterial infections caused by *N. gonorrhoeae* and *S. aureus*. For a compound to become a useful new antibiotic, it must exhibit not only high activity against pathogens but also low toxicity to the host. We are currently evaluating the fused borane−oxazoles in terms on their effects on eukaryotic cells and mice.

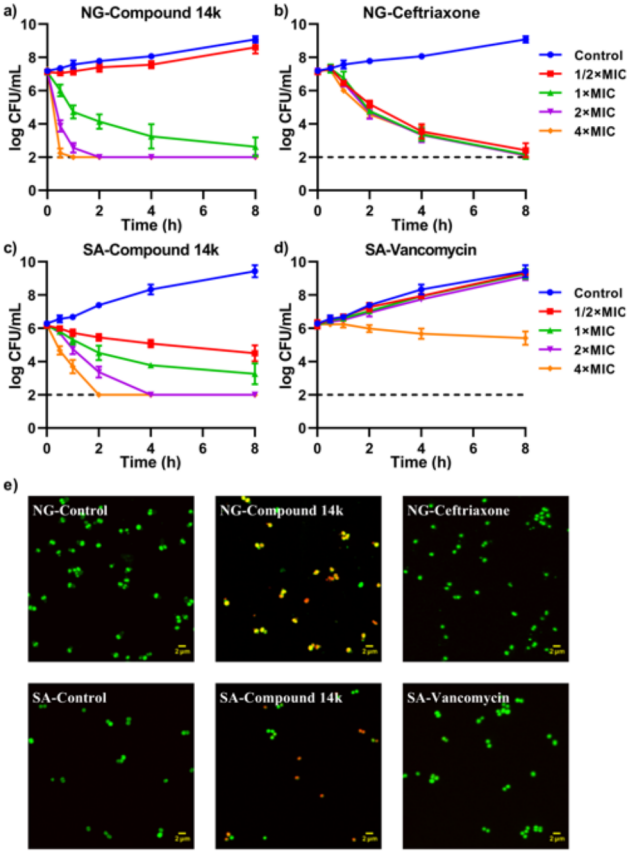

Figure 5. Bactericidal activity of compound **14k** against *Neisseria gonorrhoeae* and *Staphylococcus aureus*. Bacterial suspensions of *N. gonorrhoeae* strain ATCC 49226 (NG) and *S. aureus* strain ATCC 25923 (SA) in GC broth supplemented with 1% Vitox were incubated with compound **14k** or the control antimicrobials ceftriaxone (NG) and vancomycin (SA) at 4×, 2×, 1×, and 1/2× the minimum inhibitory concentration (MIC) or the vehicle control. Samples were taken in a time series for CFU determination or live/dead staining. (a) Survival curves of *N. gonorrhoeae* after exposure to compound **14k** (1 × MIC: 2 μM). (b) Survival curves of *N. gonorrhoeae* after exposure to ceftriaxone (1 × MIC: 0.008 μM). (c) Survival curves of *S. aureus* after exposure to compound **14k** (1 × MIC: 4 μM). (d) Survival curves of *S. aureus* after exposure to vancomycin (1 × MIC: 7 μM). Survival curves represent the mean and SD of three biological independent repeats. (e) Live/dead staining of *N. gonorrhoeae* and *S. aureus* after exposure to the vehicle control, compound **14k**, or control antibiotics ceftriaxone and vancomycin at 1× MIC for 1 h. Viable bacteria are stained with SYTO 9 (green), whereas dead bacteria are stained with propidium iodide (red) or with both SYTO 9 and propidium iodide (yellow).

CONCLUSION

An efficient synthetic protocol has been developed for the stereoselective synthesis of highly functionalized fused dodecaborate−oxazoles. The protocol is mild and allows for the rapid construction of a library of compounds in moderate to high yields and stereoselectivities. This method provides access to a previously unexplored chemical space involving the natural products menthol and camphanic acid hybridized with the $[B_{12}H_{12}]^{2-}$ cage. The evaluation of antimicrobial activity against various pathogens has resulted in the identification of several active compounds. Particularly, product **14k** exhibits potential for further drug development, as evidenced by its MIC values, time-kill assays showing bactericidal activity, and live/dead staining. These results lay the foundation for the further exploration of dodecaborate cage chirality as well as the study and improvement of antimicrobial properties of fused 2D/3D organic/inorganic heterocycle hybrid molecules.

https://doi.org/10.1021/acscentsci.1c01132
ACS Cent. Sci. 2022, 8, 322−331

■ ASSOCIATED CONTENT

Supporting Information

The Supporting Information is available free of charge at https://pubs.acs.org/doi/10.1021/acscentsci.1c01132.

Details of the synthesis and characterization of compounds, biological evaluation, spectra, and crystallographic data (PDF)

Crystallographic data for **10** (CIF)

Crystallographic data for **13a** (CIF)

■ AUTHOR INFORMATION

Corresponding Authors

Stijn van der Veen − *Department of Microbiology, and Department of Dermatology, Sir Run Run Shaw Hospital, School of Medicine, Zhejiang University, 310058 Hangzhou, People's Republic of China*; Email: stijnvanderveen@zju.edu.cn

Simon Duttwyler − *Department of Chemistry, Zhejiang University, 310027 Hangzhou, People's Republic of China*; orcid.org/0000-0001-9851-4920; Email: duttwyler@zju.edu.cn

Authors

Rajesh Varkhedkar − *Department of Chemistry, Zhejiang University, 310027 Hangzhou, People's Republic of China*; Present Address: Glenmark Life Sciences, MIDC Industrial Area, Mahape, Navi Mumbai, Maharashtra 400709, India

Fan Yang − *Department of Microbiology, and Department of Dermatology, Sir Run Run Shaw Hospital, School of Medicine, Zhejiang University, 310058 Hangzhou, People's Republic of China*

Rakesh Dontha − *Department of Chemistry, Zhejiang University, 310027 Hangzhou, People's Republic of China*; Present Address: Neuland Laboratories Ltd., Veerabhadraswamy Temple Road, Bonthapally Village, Gummadidala Mandal, Sangareddy District 502313, Telangana, India

Jianglin Zhang − *Department of Microbiology, and Department of Dermatology, Sir Run Run Shaw Hospital, School of Medicine, Zhejiang University, 310058 Hangzhou, People's Republic of China*; Present Address: Department of Biological Sciences, Carnegie Mellon University, 4400 Fifth Avenue, Pittsburgh, PA 15213, United States

Jiyong Liu − *Department of Chemistry, Zhejiang University, 310027 Hangzhou, People's Republic of China*

Bernhard Spingler − *Department of Chemistry, University of Zurich, 8057 Zurich, Switzerland*; orcid.org/0000-0003-3402-2016

Complete contact information is available at: https://pubs.acs.org/10.1021/acscentsci.1c01132

Author Contributions

‖R.V., F.Y., and R.D. contributed equally to this paper.

Author Contributions

R.V., S.v.d.V., and S.D. designed the study and wrote the paper. R.V. and R.D. synthesized and characterized all new compounds. F.Y. and J.Z. evaluated the bioactivities of all compounds. J.L. and B.S. carried out the X-ray diffraction analyses. All authors have given approval to the final version of the manuscript.

Notes

The authors declare no competing financial interest.

■ ACKNOWLEDGMENTS

Financial support by the National Natural Science Foundation of China (Nos. 21871231 and 21850410451) and the Special Funds for Basic Scientific Research of Zhejiang University (Nos. K20210335, 2019QNA3010, and 2018QNA3011) is gratefully acknowledged. The structures of **10a** and **13a** have been deposited with the Cambridge Crystallographic Data Centre (deposition numbers CCDC 2085680 and CCDC 2085681, respectively).

■ REFERENCES

(1) Spedding, M. New directions for drug discovery. *Dialogues Clin. Neurosci.* **2006**, *8*, 295−301.

(2) Morens, D. M.; Folkers, G. K.; Fauci, A. S. The challenge of emerging and re-emerging infectious diseases. *Nature* **2004**, *430*, 242−249.

(3) Brown, E. D.; Wright, G. D. Antibacterial drug discovery in the resistance era. *Nature* **2016**, *529*, 336−343.

(4) Walsh, C. Molecular mechanisms that confer antibacterial drug resistance. *Nature* **2000**, *406*, 775−781.

(5) Rossolini, G. M.; Arena, F.; Pecile, P.; Pollini, S. Update on the antibiotic resistance crisis. *Curr. Opin. Pharmacol.* **2014**, *18*, 56−60.

(6) *CDC's Antibiotic Resistance Threats in the United States*; CDC: 2019.

(7) Alanis, A. J. Resistance to Antibiotics: Are We in the Post-Antibiotic Era? *Arch. Med. Res.* **2005**, *36*, 697−705.

(8) Blair, J. M. A.; Webber, M. A.; Baylay, A. J.; Ogbolu, D. O.; Piddock, L. J. V. Molecular mechanisms of antibiotic resistance. *Nat. Rev. Microbiol.* **2015**, *13*, 42−51.

(9) Butler, M. S.; Blaskovich, M. A. T.; Cooper, M. A. Antibiotics in the clinical pipeline at the end of 2015. *J. Antibiot.* **2017**, *70*, 3−24.

(10) Newman, D. J.; Cragg, G. M. Natural Products as Sources of New Drugs from 1981 to 2014. *J. Nat. Prod.* **2016**, *79*, 629−661.

(11) Ling, L. L.; Schneider, T.; Peoples, A. J.; Spoering, A. L.; Engels, I.; Conlon, B. P.; Mueller, A.; Schäberle, T. F.; Hughes, D. E.; Epstein, S.; Jones, M.; Lazarides, L.; Steadman, V. A.; Cohen, D. R.; Felix, C. R.; Fetterman, K. A.; Millett, W. P.; Nitti, A. G.; Zullo, A. M.; Chen, C.; Lewis, K. A new antibiotic kills pathogens without detectable resistance. *Nature* **2015**, *517*, 455−459.

(12) Rutledge, P. J.; Challis, G. L. Discovery of microbial natural products by activation of silent biosynthetic gene clusters. *Nat. Rev. Microbiol.* **2015**, *13*, 509−523.

(13) Wilson, M. C.; Mori, T.; Rückert, C.; Uria, A. R.; Helf, M. J.; Takada, K.; Gernert, C.; Steffens, U. A. E.; Heycke, N.; Schmitt, S.; Rinke, C.; Helfrich, E. J. N.; Brachmann, A. O.; Gurgui, C.; Wakimoto, T.; Kracht, M.; Crüsemann, M.; Hentschel, U.; Abe, I.; Matsunaga, S.; Kalinowski, J.; Takeyama, H.; Piel, J. An environmental bacterial taxon with a large and distinct metabolic repertoire. *Nature* **2014**, *506*, 58−62.

(14) Ribeiro da Cunha, B.; Fonseca, L. P.; Calado, C. R. C. Antibiotic Discovery: Where Have We Come from, Where Do We Go? *Antibiotics* **2019**, *8*, 45−65.

(15) Aminov, R. History of antimicrobial drug discovery: Major classes and health impact. *Bioch. Pharmacol.* **2017**, *133*, 4−19.

(16) Brown, P.; Dawson, M. J.; Lawton, G.; Witty, D. R. A Perspective on the Next Generation of Antibacterial Agents Derived by Manipulation of Natural Products. *Progress in Medicinal Chemistry* **2015**, *54*, 135−184.

(17) Stokes, J. M.; Yang, K.; Swanson, K.; Jin, W.; Cubillos-Ruiz, A.; Donghia, N. M.; MacNair, C. R.; French, S.; Carfrae, L. A.; Bloom-Ackerman, Z.; Tran, V. M.; Chiappino-Pepe, A.; Badran, A. H.; Andrews, I. W.; Chory, E. J.; Church, G. M.; Brown, E. D.; Jaakkola, T. S.; Barzilay, R.; Collins, J. J. A Deep Learning Approach to Antibiotic Discovery. *Cell* **2020**, *180*, 688−702.e13.

(18) Fedorowicz, J.; Saczewski, J. Modifications of quinolones and fluoroquinolones: hybrid compounds and dual-action molecules. *Monatsh. Chem.* **2018**, *149*, 1199−1245.
(19) Stratton, C. F.; Newman, D. J.; Tan, D. S. Cheminformatic comparison of approved drugs from natural product versus synthetic origins. *Bioorg. Med. Chem. Lett.* **2015**, *25*, 4802−4807.
(20) Poater, J.; Solà, M.; Viñas, C.; Teixidor, F. Hückel's Rule of Aromaticity Categorizes Aromatic *closo*-Boron Hydride Clusters. *Chem.-Eur. J.* **2016**, *22*, 7437−7443.
(21) King, R. B. Three-Dimensional Aromaticity in Polyhedral Boranes and Related Molecules. *Chem. Rev.* **2001**, *101*, 1119−1152.
(22) *Handbook of Boron Science: With Applications in Organometallics Catalysis, Materials and Medicine*; Hosmane, N. S., Eagling, R., Eds.; World Scientific: 2018.
(23) Axtell, J. C.; Saleh, L. M. A.; Qian, E. A.; Wixtrom, A. I.; Spokoyny, A. M. Synthesis and Applications of Perfunctionalized Boron Clusters. *Inorg. Chem.* **2018**, *57*, 2333−2350.
(24) Grimes, R. N. *Carboranes*, 3rd ed.; Elsevier: 2016.
(25) Hosmane, N. S. *Boron Science: New Technologies and Applications*; Taylor & Francis Books/CRC: 2011.
(26) Sivaev, I. B.; Bregadze, V. I.; Sjöberg, S. Chemistry of *closo*-dodecaborate anion $[B_{12}H_{12}]^{2-}$: A Review. *Collect. Czech. Chem. Commun.* **2002**, *67*, 679−727.
(27) *Contemporary Boron Chemistry*; Davidson, M., Hughes, A. K., Marder, T. B., Wade, K., Eds.; Royal Society of Chemistry: 2000.
(28) Cheng, R.; Li, B.; Wu, J.; Zhang, J.; Qiu, Z.; Tang, W.; You, S. L.; Tang, Y.; Xie, Z. Enantioselective Synthesis of Chiral-at-Cage *o*-Carboranes via Pd-Catalyzed Asymmetric B−H Substitution. *J. Am. Chem. Soc.* **2018**, *140*, 4508−4511.
(29) Levit, G. L.; Krasnov, V. P.; Gruzdev, D. A.; Demin, A. M.; Bazhov, I. V.; Sadretdinova, L. S.; Olshevskaya, V. A.; Kalinin, V. N.; Cheong, C. S.; Chupakhin, O. N.; Charushin, V. N. Synthesis of *N*-[(3-amino-1,2-dicarba-*closo*-dodecaboran-1-yl)-acetyl] derivatives of alpha-amino acids. *Collect. Czech. Chem. C* **2007**, *72*, 1697−1706.
(30) Levit, G. L.; Demin, A. M.; Kodess, M. I.; Ezhikova, M. A.; Sadretdinova, L. S.; Ol'shevskaya, V. A.; Kalinin, V. N.; Krasnov, V. P.; Charushin, V. N. Acidic hydrolysis of N-acyl-1-substituted 3-amino-1,2-dicarba-*closo*-dodecaboranes. *J. Organomet. Chem.* **2005**, *690*, 2783−2786.
(31) Krasnov, V. P.; Levit, G. L.; Charushin, V. N.; Grishakov, A. N.; Kodess, M. I.; Kalinin, V. N.; Ol'shevskaya, V. A.; Chupakhin, O. N. Enantiomers of 3-amino-1-methyl-1,2-dicarba-*closo*-dodecaborane. *Tetrahedron: Asymmetry* **2002**, *13*, 1833−1835.
(32) Ali, F.; Hosmane, N. S.; Zhu, Y. Boron Chemistry for Medical Applications. *Molecules* **2020**, *25*, 828−851.
(33) Silva, M. P.; Saraiva, L.; Pinto, M.; Sousa, M. E. Boronic Acids and Their Derivatives in Medicinal Chemistry: Synthesis and Biological Applications. *Molecules* **2020**, *25*, 4323−4362.
(34) Viñas, C.; Núñez, R.; Bennour, I.; Teixidor, F. Periphery Decorated and Core Initiated Neutral and Polyanionic Borane Large Molecules: Forthcoming and Promising Properties for Medicinal Applications. *Curr. Med. Chem.* **2019**, *26*, 5036−5076.
(35) Yinghuai, Z.; Lin, X.; Xie, H.; Li, J.; Hosmane, N. S.; Zhang, Y. The Current Status and Perspectives of Delivery Strategy for Boron-based Drugs. *Curr. Med. Chem.* **2019**, *26*, 5019−5035.
(36) Trippier, P. C.; McGuigan, C. Boronic Acids in Medicinal Chemistry: Anticancer, Antibacterial and Antiviral Applications. *Medchemcomm* **2010**, *1*, 183−198.
(37) Richardson, P. G.; Hideshima, T.; Anderson, K. C. Bortezomib (PS-341): a novel, first-in-class proteasome inhibitor for the treatment of multiple myeloma and other cancers. *Cancer Control* **2003**, *10*, 361−369.
(38) Hecker, S. J.; Raja Reddy, K.; Lomovskaya, O.; Griffith, D. C.; Rubio-Aparicio, D.; Nelson, K.; Tsivkovski, R.; Sun, D.; Sabet, M.; Tarazi, Z.; Parkinson, J.; Totrov, M.; Boyer, S. H.; Glinka, T. W.; Pemberton, O. S.; Chen, Y.; Dudley, M. N. Discovery of Cyclic Boronic Acid QPX7728, an Ultrabroad-Spectrum Inhibitor of Serine and Metallo-*β*-lactamases. *J. Med. Chem.* **2020**, *63*, 7491−7507.
(39) Leśnikowski, Z. J. Challenges and Opportunities for the Application of Boron Clusters in Drug Design. *J. Med. Chem.* **2016**, *59*, 7738−7758.
(40) Gabel, D. Boron clusters in medicinal chemistry: perspectives and problems. *Pure Appl. Chem.* **2015**, *87*, 173−179.
(41) Scholz, M.; Hey-Hawkins, E. Carbaboranes as Pharmacophores: Properties, Synthesis, and Application Strategies. *Chem. Rev.* **2011**, *111*, 7035−7062.
(42) Issa, F.; Kassiou, M.; Rendina, L. M. Boron in Drug Discovery: Carboranes as Unique Pharmacophores in Biologically Active Compounds. *Chem. Rev.* **2011**, *111*, 5701−5722.
(43) Valliant, J. F.; Guenther, K. J.; King, A. S.; Morel, P.; Schaffer, P.; Sogbein, O. O.; Stephenson, K. A. The medicinal chemistry of carboranes. *Coord. Chem. Rev.* **2002**, *232*, 173−230.
(44) Fink, K.; Uchmann, M. Boron cluster compounds as new chemical leads for antimicrobial therapy. *Coord. Chem. Rev.* **2021**, *431*, 213684−213693.
(45) Plešek, J. Potential Applications of the Boron Cluster Compounds. *Chem. Rev.* **1992**, *92*, 269−278.
(46) Zheng, Y.; Liu, W. W.; Chen, Y.; Jiang, H.; Yan, H.; Kosenko, I.; Chekulaeva, L.; Sivaev, I.; Bregadze, V.; Wang, X. M. A Highly potent antibacterial agent targeting methicillin-resistant staphylococcus aureus based on cobalt bis(1,2-dicarbollide) alkoxy derivative. *Organometallics* **2017**, *36*, 3484−3490.
(47) Romero, I.; Martinez-Medina, M.; Camprubí-Font, C.; Bennour, I.; Moreno, D.; Martínez-Martínez, L.; Teixidor, F.; Fox, M. A.; Viñas, C. Metallacarborane Assemblies as Effective Antimicrobial Agents, Including a Highly Potent Anti-MRSA Agent. *Organometallics* **2020**, *39*, 4253−4264.
(48) Vaňková, E.; Lokočová, K.; Maťátková, O.; Krízŏvá, I.; Masák, J.; Grüner, B.; Kaule, P. Čermák, J.; Šícha, V. Cobaltbis-dicarbollide and its ammonium derivatives are effective antimicrobial and antibiofilm agents. *J. Organomet. Chem.* **2019**, *899*, 120891−120898.
(49) Kvasničková, E.; Masák, J.; Čejka, J.; Maťátková, O.; Šícha, V. Preparation, characterization, and the selective antimicrobial activity of N-alkylammonium 8-diethyleneglycol cobalt bis-dicarbollide derivatives. *J. Organomet. Chem.* **2017**, *827*, 23−31.
(50) Popova, T.; Zaulet, A.; Teixidor, F.; Alexandrova, R.; Viñas, C. Investigations on antimicrobial activity of cobaltabisdicarbollides. *J. Organomet. Chem.* **2013**, *747*, 229.
(51) Stauber, J. M.; Qian, E. A.; Han, Y.; Rheingold, A. L.; Král, P.; Fujita, D.; Spokoyny, A. M. An Organometallic Strategy for Assembling Atomically Precise Hybrid Nanomaterials. *J. Am. Chem. Soc.* **2020**, *142*, 327−334.
(52) Sun, Y.; Zhang, J.; Zhang, Y.; Liu, J.; van der Veen, S.; Duttwyler, S. The *closo*-Dodecaborate Dianion Fused with Oxazoles Provides 3D Diboraheterocycles with Selective Antimicrobial Activity. *Chem.-Eur. J.* **2018**, *24*, 10364−10371.
(53) Hamdaoui, M.; Varkhedkar, R.; Sun, J.; Fan, L.; Duttwyler, S. Recent advances in the selective functionalization of anionic icosahedral boranes and carboranes. In *Synthetic Inorganic Chemistry*; Hamilton, E. J. M., Hosmane, N. S., Eds.; Elsevier: 2021; pp 343−389.
(54) Quan, Y.; Xie, Z. Controlled functionalization of *o*-carborane via transition metal catalyzed B−H activation. *Chem. Soc. Rev.* **2019**, *48*, 3660−3673.
(55) Zhang, X.; Yan, H. Transition metal-induced B−H functionalization of o-carborane. *Coord. Chem. Rev.* **2019**, *378*, 466−482.
(56) Duttwyler, S. Recent advances in B−H functionalization of icosahedral carboranes and boranes by transition metal catalysis. *Pure Appl. Chem.* **2018**, *90*, 733−744.
(57) Quan, Y.; Qiu, Z.; Xie, Z. Transition-Metal-Catalyzed Selective Cage B−H Functionalization of *o*-Carboranes. *Chem.-Eur. J.* **2018**, *24*, 2795−2805.
(58) Yu, W.-B.; Cui, P.-F.; Gao, W.-X.; Jin, G.-X. B−H activation of carboranes induced by late transition metals. *Coord. Chem. Rev.* **2017**, *350*, 300−319.
(59) Shen, Y.; Zhang, K.; Liang, X.; Dontha, R.; Duttwyler, S. Highly selective palladium-catalyzed one-pot, five-fold B−H/C−H cross

https://doi.org/10.1021/acscentsci.1c01132
ACS Cent. Sci. 2022, 8, 322−331

coupling of monocarboranes with alkenes. *Chem. Sci.* **2019**, *10*, 4177−4184.
(60) Lin, F.; Yu, J.-Lu; Shen, Y.; Zhang, S.-Q.; Spingler, B.; Liu, J.; Hong, X.; Duttwyler, S. Palladium-Catalyzed Selective Five-Fold Cascade Arylation of the 12-Vertex Monocarborane Anion by B−H Activation. *J. Am. Chem. Soc.* **2018**, *140*, 13798−13807.
(61) Zhang, Y.; Wang, T.; Wang, L.; Sun, Y.; Lin, F.; Liu, J.; Duttwyler, S. Rh(III)-Catalyzed Functionalization of *closo*-Dodecaborates by Selective B−H Activation: Bypassing Competitive C−H Activation. *Chem.-Eur. J.* **2018**, *24*, 15812−15817.
(62) Lin, F.; Shen, Y.; Zhang, Y.; Sun, Y.; Liu, J.; Duttwyler, S. Fusing Carborane Carboxylic Acids with Alkynes: 3D Analogues of Isocoumarins via Regioselective B−H Activation. *Chem.-Eur. J.* **2018**, *24*, 551−555.
(63) Shen, Y.; Pan, Y.; Zhang, K.; Liang, X.; Liu, J.; Spingler, B.; Duttwyler, S. B−H functionalization of the monocarba-*closo*-dodecaborate anion by rhodium and iridium catalysis. *Dalton Trans.* **2017**, *46*, 3135−3140.
(64) Zhang, Y.; Sun, Y.; Lin, F.; Liu, J.; Duttwyler, S. Rhodium(III)-Catalyzed Alkenylation−Annulation of *closo*-Dodecaborate Anions through Double B−H Activation at Room Temperature. *Angew. Chem., Int. Ed.* **2016**, *55*, 15609−15614.
(65) Chen, W.; Vermaak, I.; Viljoen, A. Camphor − a fumigant during the Black Death and a coveted fragrant wood in ancient Egypt and Babylon − a review. *Molecules* **2013**, *18*, 5434−5454.
(66) İşcan, G.; Kirimer, N.; Kürkcüoğlu, M. N.; Hüsnü Can, B.; Demirci, F. H. Antimicrobial Screening of Mentha piperita Essential Oils. *J. Agr. Food Chem.* **2002**, *50*, 3943−3946.
(67) The amount of R_{cage} single crystals of **13a** was not high enough for an NMR analysis, and crystallization of this and other compounds generally proved difficult. The chromatographic separation of diastereomers was also not successful.
(68) Tacconelli, E.; Carrara, E.; Savoldi, A.; Harbarth, S.; Mendelson, M.; Monnet, D. L.; Pulcini, C.; Kahlmeter, G.; Kluytmans, J.; Carmeli, Y.; Ouellette, M.; Outterson, K.; Patel, J.; Cavaleri, M.; Cox, E. M.; Houchens, C. R.; Grayson, M. L.; Hansen, P.; Singh, N.; Theuretzbacher, U.; Magrini, N. WHO Pathogens Priority List Working Group. Discovery, research, and development of new antibiotics: the WHO priority list of antibiotic-resistant bacteria and tuberculosis. *Lancet Infect. Dis.* **2018**, *18*, 318−327.
(69) Yang, F.; Yan, J.; van der Veen, S. Antibiotic Resistance and Treatment Options for Multidrug-Resistant Gonorrhea. *Infect. Microb. Dis.* **2020**, *2*, 67−76.
(70) Unemo, M.; Shafer, W. M. Antimicrobial resistance in *Neisseria gonorrhoeae* in the 21st century: past, evolution, and future. *Clin. Microbiol. Rev.* **2014**, *27*, 587−613.
(71) Gransden, W. R.; Warren, C. A.; Phillips, I.; Hodges, M.; Barlow, D. Decreased susceptibility of *Neisseria gonorrhoeae* to ciprofloxacin. *Lancet* **1990**, *335*, 51.
(72) Starnino, S.; Galarza, P.; Carvallo, M. E.; Benzaken, A. S.; Ballesteros, A. M.; Cruz, O. M.; Hernandez, A. L.; Carbajal, J. L.; Borthagaray, G.; Payares, D.; Dillon, J. A. Retrospective analysis of antimicrobial susceptibility trends (2000−2009) in *Neisseria gonorrhoeae* isolates from countries in Latin America and the Caribbean shows evolving resistance to ciprofloxacin, azithromycin and decreased susceptibility to ceftriaxone. *Sex Transm. Dis.* **2012**, *39*, 813−821.
(73) Ni, C.; Xue, J.; Zhang, C.; Zhou, H.; van der Veen, S. High prevalence of *Neisseria gonorrhoeae* with high-level resistance to azithromycin in Hangzhou, China. *J. Antimicrob. Chemother.* **2016**, *71*, 2355−2357.
(74) Fifer, H.; Hughes, G.; Whiley, D.; Lahra, M. M. Lessons learnt from ceftriaxone-resistant gonorrhoea in the UK and Australia. *Lancet Infect. Dis.* **2020**, *20*, 276−278.
(75) Yan, J.; Chen, Y.; Yang, F.; Ling, X.; Jiang, S.; Zhao, F.; Yu, Y.; van der Veen, S. High percentage of the ceftriaxone-resistant *Neisseria gonorrhoeae* FC428 clone among isolates from a single hospital in Hangzhou, China. *J. Antimicrob. Chemother.* **2021**, *76*, 936−939.
(76) (a) Pankey, G. A.; Sabath, L. D. Clinical relevance of bacteriostatic versus bactericidal mechanisms of action in the treatment of Gram-positive bacterial infections. *Clin. Infect. Dis.* **2004**, *38*, 864−870.
(77) Finberg, R. W.; Moellering, R. C.; Tally, F. P.; Craig, W. A.; Pankey, G. A.; Dellinger, E. P.; West, M. A.; Joshi, M.; Linden, P. K.; Rolston, K. V.; Rotschafer, J. C.; Rybak, M. J. The importance of bactericidal drugs: future directions in infectious disease. *Clin. Infect. Dis.* **2004**, *39*, 1314−1320.
(78) Liu, C.; Bayer, A.; Cosgrove, S. E.; Daum, R. S.; Fridkin, S. K.; Gorwitz, R. J.; Kaplan, S. L.; Karchmer, A. W.; Levine, D. P.; Murray, B. E.; Rybak, M.; Talan, D. A.; Chambers, H. F. Infectious Diseases Society of America. Clinical practice guidelines by the infectious diseases society of America for the treatment of methicillin-resistant Staphylococcus aureus infections in adults and children. *Clin. Infect. Dis.* **2011**, *52*, e18−55.

https://doi.org/10.1021/acscentsci.1c01132
ACS Cent. Sci. 2022, 8, 322−331